Journal of Visualized Experiments
Application of Optical Coherence Tomography to a Mouse Model of Retinopathy
--Manuscript Draft--

Article Type:	Invited Methods Article - JoVE Produced Video
Manuscript Number:	JoVE63421R3
Full Title:	Application of Optical Coherence Tomography to a Mouse Model of Retinopathy
Corresponding Author:	Xiaoting Mai, Ph.D. Joint Shantou International Eye Center of Shantou University and The Chinese University of Hong Kong Shantou, Guangdong CHINA
Corresponding Author's Institution:	Joint Shantou International Eye Center of Shantou University and The Chinese University of Hong Kong
Corresponding Author E-Mail:	373173543@qq.com
Order of Authors:	Xiaoting Mai, Ph.D.
	Shaofen Huang
	Wen Chen
	Tsz Kin Ng
	Haoyu Chen
Additional Information:	
Question	**Response**
Please specify the section of the submitted manuscript.	Medicine
Please indicate whether this article will be Standard Access or Open Access.	Standard Access ($1400)
Please indicate the **city, state/province, and country** where this article will be **filmed**. Please do not use abbreviations.	Shantou city, Guangdong province, China
Please confirm that you have read and agree to the terms and conditions of the author license agreement that applies below:	I agree to the Author License Agreement
Please confirm that you have read and agree to the terms and conditions of the video release that applies below:	I agree to the Video Release
Please provide any comments to the journal here.	no

TITLE:
Application of Optical Coherence Tomography to a Mouse Model of Retinopathy

AUTHORS AND AFFILIATIONS:
Xiaoting Mai[1,#], Shaofen Huang[1,#], Wen Chen[1], Tsz Kin Ng[1-3], Haoyu Chen[1]

[1]Joint Shantou International Eye Center, Shantou University and the Chinese University of Hong Kong, Shantou, Guangdong, China
[2]Shantou University Medical College, Shantou, Guangdong, China
[3]Department of Ophthalmology and Visual Sciences, the Chinese University of Hong Kong, Hong Kong

[#]These authors are co-first authors.

Email addresses of co-authors:
Xiaoting Mai   (373173543@qq.com)
Shaofen Huang   (hsf@jsiec.org)
Wen Chen   (chenwen@jsiec.org)
Tsz Kin Ng   (micntk@hotmail.com)

Corresponding author:
Haoyu Chen   (chy@jsiec.org)

SUMMARY:
Here, we describe an *in vivo* imaging technique using optical coherence tomography to facilitate the diagnosis and quantitative measurement of retinopathy in mice.

ABSTRACT:
Optical coherence tomography (OCT) offers a noninvasive method for the diagnosis of retinopathy. The OCT machine can capture retinal crosssectional images from which the retinal thickness can be calculated. Although OCT is widely used in clinical practice, its application in basic research is not as prevalent, especially in small animals such as mice. Because of the small size of their eyeballs, it is challenging to conduct fundus imaging examinations in mice. Therefore, a specialized retinal imaging system is required to accommodate OCT imaging on small animals. This article demonstrates a small-animal-specific system for OCT examination procedures and a detailed method for image analysis. The results of retinal OCT examination of very-low-density lipoprotein receptor (*Vldlr*) knockout mice and C57BL/6J mice are presented. The OCT images of C57BL/6J mice showed retinal layers, while those of *Vldlr* knockout mice showed subretinal neovascularization and retinal thinning. In summary, OCT examination could facilitate the noninvasive detection and measurement of retinopathy in mouse models.

INTRODUCTION:
Optical coherence tomography (OCT) is an imaging technique that can provide *in vivo* high resolution and crosssectional imaging for tissue[1-8], especially for the noninvasive examination in

45   the retina[9-12]. It can also be used to quantify some important biomarkers, such as retinal thickness
46   and retinal nerve fiber layer thickness. The principle of OCT is optical coherence reflectometry,
47   which obtains crosssectional tissue information from the coherence of light reflected from a
48   sample and converts it into a graphic or digital form through a computer system[7]. OCT is widely
49   used in ophthalmology clinics as an essential tool for diagnosis, follow-up, and management for
50   patients with retinal disorders. It can also provide insight into the pathogenesis of retinal diseases.
51
52   In addition to clinical applications, OCT has also been used in animal studies. Although pathology
53   is the gold standard of morphological characterization, OCT has the advantage of noninvasive *in*
54   *vivo* imaging and longitudinal follow-up. Furthermore, it has been shown that OCT is well
55   correlated with histopathology in retinopathy animal models[11,13-20]. The mouse is the most
56   commonly used animal in biomedical studies. However, its small eyeballs pose a technical
57   challenge to conducting OCT imaging in mice.
58
59   Compared to the OCT first used for retinal imaging in mice[21,22], OCT in small animals has now
60   been optimized with respect to hardware and software systems. For example, OCT, in
61   combination with the tracker, significantly reduces the signal-to-noise ratio; OCT software system
62   upgrades allow more retinal layers to be detected automatically; and the integrated DLP beamer
63   helps to reduce the motion artifacts.
64
65   Very-low-density lipoprotein receptor (Vldlr) is a transmembrane protein in endothelial cells. It
66   is expressed on retinal vascular endothelial cells, retinal pigment epithelial cells, and around the
67   outer limiting membrane[23,24]. Subretinal neovascularization is the phenotype of *Vldlr* knockout
68   mice[23]. Therefore, *Vldlr* knockout mice are used to investigate the pathogenesis and potential
69   therapy of subretinal neovascularization. This article demonstrates the application of OCT
70   imaging to detect retinal lesions in *Vldlr* knockout mice, hoping to provide some technical
71   reference for retinopathy research in small animal models.
72
73   **PROTOCOL:**
74
75   The operations were performed following the Statement on the Use of Animals in Ophthalmic
76   and Vision research from the Association for Research in Vision and Ophthalmology. The
77   experimental design was approved by the institutional animal Ethics Committee. Two-month-old
78   C57/BL/6J mice and *Vldlr* knockout mice were used in this study. There were 7 mice in each group,
79   all of which were female and weighed 20 g to 24 g.
80
81   **1.   Experimental conditions**
82
83   1.1.   Assign the mice to two groups: an experimental group consisting of *Vldlr* knockout mice
84   and a control group consisting of C57BL/6J mice.
85
86   1.2.   Feed the mice with food and water conventionally.
87
88   1.3.   Raise the mice in the animal laboratory under stable conditions of room temperature

89 (22 °C), humidity (50–60%), light–dark cycle (12 h–12 h), and room light intensity (350–400 lux).

90

91 1.4.   Prepare the experimental equipment: optical coherence tomography with confocal
92 scanning laser ophthalmoscope (cSLO) for small animals (**Figure 1A**).

93

94 1.5.   Prepare all materials required for the experiment (**Figure 1B**) and weigh the mice (**Figure**
95 **1C**).

96

97 **2.   Anesthetic configuration**

98

99 2.1.   Add 3.57 mL of sterilized water to a bottle of lyophilized anesthetic powder (Tiletamine
100 125 mg + Zolazepam 125 mg) to achieve a final concentration of 70 mg/mL.

101

102 2.2.   Dissolve 200 mg of Xylazine powder in 10 mL of sterilized water to a final concentration
103 of 20 mg/mL.

104

105 2.3.   Mix the two solutions in a new tube (take the same volume to mix, volume ratio 1:1);

106

107 2.4.   Set the injection dosage of the anesthetic mixture solution as 1 µL/g.

108

109 NOTE: Dosage selection should be according to the experiment duration. When the dosage is 1
110 µL/g (1 µL of anesthetic mixture for each 1 g weight of mouse), the duration of deep anesthesia
111 is ~1 h. When the dosage is 1.5 µL/g (1.5 µL of anesthetic mixture for each 1 g weight of mice),
112 the duration of deep anesthesia is ~2 h. The dosage of 1 µL/g anesthetic mixture met the time
113 requirement of OCT (0.5–1 h) for one mouse.

114

115 **3.   Information records**

116

117 3.1.   Record the information: group, code, date of birth, age, sex, weight, and anesthetic
118 dosage.

119

120 **4.   Instrument startup and testing**

121

122 4.1.   Switch on the computer and start up the software.

123

124 4.2.   Click the **Test program** button to complete the test program.

125

126 4.3.   Turn on the thermostat and preheat it to the temperature of 37 °C.

127

128 4.4.   Start the **OCT module** procedure after the program testing.

129

130 4.5.   Create a new subject and fill in the mouse information.

131

132 4.6.   Preheat the electric blanket and cover it with surgical towels.

5. Application of mydriatic drops

135

5.1.   Grab the mouse, pull the neck fur, make the eyeball protrude slightly, and rotate the mouse head with one eye facing upward.

138

5.2.   Apply the mydriatic drops to the eyes to dilate the pupil, one drop in each eye (**Figure 2A**).

140

5.3.   Rotate the head to add the mydriatic eye drop to the other eye.

142

5.4.   Wipe away any excess liquid spilling over the face.

144

5.5.   Check for pupil dilation after 10 min.

146

6.   Anesthesia: Intramuscular injection (after pupil dilation)

148

6.1.   Calculate the injection volume of the anesthetic mixture solution according to the weight, e.g., 20 µL/20 g (**Figure 1C**).

151

6.2.   Extract the corresponding volume of the anesthetic mixture with a 50 µL microsyringe, e.g., 20 µL.

154

6.3.   Select the lateral thigh muscles of the mouse as the injection point.

156

6.4.   Remove the localized hair with scissors to expose the thigh muscles.

158

6.5.   Disinfect the skin three times with povidone-iodine (**Figure 1B–I** and **Figure 2B**).

160

6.6.   Insert the microsyringe needle into the muscle at an angle of 60–90° with the bevel of the needle mouth facing upwards and a depth of ~0.3 cm (ensure that the bevel is fully inserted into the muscle; **Figure 2C**).

164

6.7.   Inject all of the anesthetic solution in the microsyringe (**Figure 2C**).

166

NOTE: A smooth injection with no spillover indicates successful injection.

168

6.8.   Pull out the needle quickly after injection.

170

6.9.   Press the injection area with a cotton swab for 30 s.

172

6.10.   Ensure that there is no local bleeding and congestion.

174

7.   Placement of the mouse

176

177 7.1.   Place a mouse on an electric blanket platform.
178
179 7.2.   Coat both eyes with medical sodium hyaluronate gel immediately after anesthesia (**Figure**
180 **2D**).
181
182 7.3.   Screw a 60 D double spherical lens (preset lens) on the cSLO device (**Figure 1A–5,6**).
183
184 7.4.   Place a 100 D contact lens on the mouse cornea with the concave side touching the
185 sodium hyaluronate gel on the corneal surface (**Figure 2E,F** and **Figure 3A–II**).
186
187 7.5.   Place the mouse on the small, constant-temperature animal platform and keep the eye
188 1–2 mm away from the lens of the cSLO device (**Figure 3A**).
189
190 7.6.   Adjust the angle of the contact lens with forceps to keep the pupil in the center of the
191 lens.
192
193 7.7.   Fine-tune the adjustments to the head to make the eye face straight ahead.
194
195 **8.**   **Confocal Scanning Laser Ophthalmoscope (cSLO)**
196
197 8.1.   Click the **OCT** button, choose the **mouse** module, and start the **cSLO** program (**Figure 4B**).
198
199 8.2.   Select the **IR** mode (**light source: red light**), and adjust the parameter (**range: 2047, Figure**
200 **4D**).
201
202 8.3.   Select the eye to be examined (right eye: **Figure 4C-1**; left eye: **Figure 4C-2**)
203
204 8.4.   Control the lever and move the preset lens towards the contact lens slowly.
205
206 8.5.   Adjust the diopter value until the posterior pole imaging is clear (**Figure 4E**).
207
208 8.6.   Make further adjustments to align the image of the retinal posterior pole, centering it at
209 the optic nerve head.
210
211 **9.**   **Optical coherence tomography (OCT)**
212
213 9.1.   Start the OCT program (**Figure 4G**).
214
215 9.2.   Click the progress bar up and down until the OCT image appears (**Figure 4H**).
216
217 9.3.   Adjust parameters: Range Min (**Figure 4I**) = 0–20, Range Max (**Figure 4J**) = 50–60.
218
219 9.4.   Adjust the preset lens distance and position direction until an ideal OCT image is obtained.
220

221   9.5.   Select the scanning position by moving the standard line in the cSLO (**Figure 4M**).

223   9.6.   Start scanning from the optic nerve head.

225   9.7.   Collect images in the same order for each eye: horizontal line: optic nerve head →
226   superior → inferior; vertical line: optic nerve head → nasal → temporal.

228   9.8.   Collect images from four directions.

230   9.9.   Click **Average** to overlay the cSLO and OCT image signals (**Figure 4F** and **Figure 4O**).

232   9.10.   Click the **shot** button to acquire the SLO-OCT image (**Figure 4P**).

234   9.11.   Save and export all the images (**Figure 4Q, R**).

236   **10. The end of the experiment (after the OCT examination)**

238   10.1.   Place the mouse on the electric blanket to keep it warm until it wakes up.

240   NOTE: The mouse should be monitored until it regains sufficient consciousness to maintain
241   sternal recumbency.

243   10.2.   Remove the 100 D contact lens.

245   10.3.   Apply the levofloxacin eye gel to protect the cornea.

247   10.4.   Place the mouse back in the cage after it wakes up.

249   NOTE: Ensure that the examined mouse is not returned to the company of other mice until fully
250   recovered.

252   10.5.   Turn off the software and switch off the computer.

254   10.6.   Clean the 100 D contact lens with water; dry the lens.

256   10.7.   Clean and disinfect the environment.

258   **11.   Image analysis**

260   11.1.   Compare the OCT images of *Vldlr* knockout mice with those of C57BL/6J mice.

262   11.2.   Observe multiple positions: vertical and horizontal scans passing through the optic papilla;
263   superior, inferior, nasal, and temporal scans; and abnormal reflection site scans.
264

265   11.3.   Observe the thickness, shape, layering, and abnormal reflectance lesions of the retina in
266   each image, as well as the vitreous interface of the retina and the vitreous body.

267

268   11.4.   Record the locations, characteristics, and numbers of lesions.

269

270   **12. Retinal stratification correction**

271

272   12.1.   Click **Load Examination** on the OCT interface (**Figure 5A**).

273

274   12.2.   Call out the OCT images of a mouse from a pop-up window.

275

276   12.3.   Select images: OCT image scanning through the optic papilla, horizontally or vertically.

277

278   12.4.   Double-click the image in the **Media Container** to display it on the screen (**Figure 5C**).

279

280   12.5.   Click on **Layer Detection** to complete automatic layering on the retina (**Figure 5D**).

281

282   12.6.   Select the dividing lines on both sides of the layer prepared for analysis (**Figure 6D–10**).

283

284   12.7.   Select a separate dividing line (**Figure 6B-6**) and click **Edit Layer** (**Figure 6A–1**) to activate
285   the line when a red circle appears (**Figure 6B-7**).

286

287   12.8.   Adjust **Spacing** (**Figure 6A–4, e.g., 50**) and **Limit Range** (**Figure 6A–5, e.g., 50**).

288

289   12.9.   Modify the dividing line by moving the red circle (compare the green dividing line in **Figure
290   6B** and **Figure 6C**; **Figure 6C** shows the modified result).

291

292   **13.   Retinal lamination thickness**

293

294   13.1.   Click the **Measure Marker** button (**Figure 6D–9**).

295

296   13.2.   Select the dividing line of the layer to be analyzed (e.g., in the outer nuclear layer, select
297   the 4th and 5th dividing line in the list) to display the boundary of the layer on the OCT image
298   (**Figure 6D–10**).

299

300   13.3.   Select **Connect with Layer** (**Figure 6D–11**) and **Stay Connected on Move** (**Figure 6D–12**).

301

302   13.4.   Select the area to display the results (the selected column is colored, **Figure 6D–13**).

303

304   13.5.   Click the position to be analyzed on the OCT image to make the measurement line appear
305   (perpendicular to the horizontal axis and consistent with the color of the resulting area) (**Figure
306   6D–14**).

307

308   13.6.   Click on the next column for the next measurement and reveal the previous data (**Figure**

309   6E–15).

311   13.7.   Read the **Vert** value (thickness of the measured position) in the **Length in µm (tissue)** row
312   (**Figure 6E, red rectangle**).

314   13.8.   Click **Delete Marker** (**Figure 6E–16**) and **New Marker** (**Figure 6E–17**) to retest so that the
315   results will cover the original data (if remeasurement is necessary).

317   13.9.   Press **Print Scr** on the keyboard to save screenshots, or click **Save Examination** to save
318   directly (**Figure 5H**).

320   13.10. Input the data into a spreadsheet or statistical software for statistical analysis.

322   **14.   Measurement of full retinal thickness**

324   14.1.   Select **line 1** (**ILM**, inner limiting membrane, **Figure 7B**) and **line 7** (**OS-RPE**, OS: outer
325   photoreceptor segments; RPE: retinal pigment epithelial layer, **Figure 7C**) in the list in the upper
326   right corner.

328   NOTE: The full retinal thickness means the thickness of the retinal neurepithelium layer, which is
329   the retina between ILM and OS-RPE on OCT).

331   14.2.   Measure the retinal thickness on both sides of the optic papilla at a specific interval.

333   14.2.1. For example: from the appearance of the retinal structure at the edge of the optic papilla,
334   measure 4 values with 200 µm spacing of the horizontal ruler (**Figure 7G,H**).

336   14.3.   Record all measured values in a spreadsheet.

338   14.4.   Use multiple *t*-tests (one per row) to compare the measured values of each corresponding
339   position in both groups.

341   **REPRESENTATIVE RESULTS:**
342   Thanks to the high-resolution scans of OCT, the layers of the mouse retina can be observed, and
343   abnormal reflections and their exact locations can be identified. The retinal OCT images of *Vldlr*
344   knockout mice and C57BL/6J mice were compared in this study. The OCT images of all C57BL/6J
345   mice showed various retinal layers with different reflectivity, and the demarcation was clear
346   (**Figure 8D**). In contrast, all *Vldlr* knockout mice showed abnormal, hyperreflective lesions on the
347   OCT images (**Figure 8B**).

349   **Incomplete vitreous detachment (PVD) in *Vldlr* knockout mice**
350   The OCT results showed some middle reflective bands on the retinal surfaces of *Vldlr* knockout
351   mice (**Figure 8B, red arrows**). These middle reflective bands adhered to the retinal vessel (**Figure
352   8B, green arrow**), corresponding to the cSLO image (**Figure 8A, green arrow**). These features are

353 consistent with the OCT characteristics of incomplete vitreous detachment.
354

355 **Subretinal neovascularization in *Vldlr* knockout mice**
356 The results showed that subretinal neovascularization had two development modes in the *Vldlr*
357 knockout mice.
358

359 **With involvement of the outer nuclear layer**
360 A hyperreflective lesion, with a bottom-down triangular shape on the OCT image, appeared on
361 the subretinal space and spread to the outer nuclear layer. The lesion did not break through the
362 outer plexiform layer (**Figure 8B, white arrow**).
363

364 The OCT appearance of this type of subretinal neovascularization was consistent with the
365 pathological findings shown in **Figure 9A**. The pathological section showed that
366 neovascularization (**Figure 9A, thick green arrow**) broke through the RPE, photoreceptor
367 inner/outer segments (IS/OS), and the external limiting membrane (ELM). It invaded the outer
368 nuclear layer (ONL) but did not break through the outer plexiform layer (OPL).
369

370 **Without involvement of the outer nuclear layer**
371 A band of hyperreflective lesion appeared on the OCT image, which was located at the subretinal
372 space (**Figure 8B, yellow arrow**). The cSLO image showed the corresponding location (**Figure 8A,
373 yellow arrow**). The additional scans of the retina around this location (**Figure 8A, yellow arrow**)
374 showed the same findings.
375

376 Consistent with the lesion (**Figure 10A, thick blue arrow**) in the pathological section, this
377 subretinal neovascularization did not break through the ELM (**Figure 10A, thin yellow arrow**) but
378 partially involved the photoreceptor IS/OS.
379

380 **Retinal thickness results**
381 The retinal thickness of the right eye of all mice was obtained by using the automatic stratification
382 and thickness measurement function of OCT. The retinal thickness of *Vldlr* knockout mice (200.94
383 ± 14.64 µm) was significantly lower than that of C57BL/6J mice (217.46 ± 10.21 µm, P < 0.001, *t*-
384 test, 7 right eyes/group). The comparison of retinal thickness in the four directions (temporal,
385 nasal, superior, and inferior) of the posterior polar between the two groups is shown in **Figure
386 11**.
387

388 **FIGURE AND TABLE LEGENDS:**
389

390 **Figure 1: Preparation of experimental materials and animals.** (**A**) Equipment: 1. cSLO/OCT
391 device for small-animal retinal imaging, 2. computer and monitor, 3. Small, constant-temperature
392 animal platform, 4. thermostat, 5. preset lens, 6. installation of the preset lens. (**B**) Medicines and
393 small items: I. povidone-iodine, II. microsyringe, III. anesthetic mixture solution, IV. timer, V.
394 mydriatic eye drops, VI. forceps, VII. medical sodium hyaluronate gel, VIII. medical cotton swab,
395 IX. antibiotic eye ointment, X. 100 D contact lens (two). (**C**) Weight measurement on a digital
396 balance. Abbreviations: cSLO = confocal scanning laser ophthalmoscope; OCT = optical coherence

397   tomography.

398

399   **Figure 2: Preparation before OCT examination of mice.** (**A**) Mydriasis eye drop application, (**B**)
400   disinfection at the anesthetic injection site with povidone-iodine, (**C**) intramuscular injection of
401   the anesthetic drug, (**D**) sodium hyaluronate gel coating on the cornea, (**E, F**) placement of a 100
402   D contact lens, with concave surface contacting the cornea. Abbreviation: OCT = optical
403   coherence tomography.

404

405   **Figure 3: OCT examination procedures.** (**A**) Mouse position placement, I. preset lens, II. contact
406   lens, III. Small, constant-temperature animal platform. (**B**) Operation of the cSLO/OCT machine,
407   IV. operating lever, V. tilt lever, VI. cSLO device. Abbreviations: cSLO = confocal scanning laser
408   ophthalmoscope; OCT = optical coherence tomography.

409

410   **Figure 4: OCT imaging process.** A. **Measurement** mode, B. **Start Lase**r of the IR laser, C. eye
411   selection (C-1-OD; C-2-OS), D. range of IR laser, E. the diopter, F. overlay of the cSLO image, G.
412   OCT scanning start/stop laser button H. reference of OCT image, I. **Range Min**: 0–20, J. **Range**
413   **Max**: 50–60, K. signal intensity of the image, L. scanning direction (e.g., vertical scan), M. scanning
414   position selected by moving the green reference line (e.g., vertical scan through the optic papilla),
415   N. real-time display of the OCT image, O. overlay of the OCT image, P. **Shot**: image acquisition, Q.
416   SLO-OCT images that have been acquired, R. **Save Examination**: saving the examination result.
417   Scale bars = 200 μm. Abbreviations: cSLO = confocal scanning laser ophthalmoscope; OCT =
418   optical coherence tomography; IR = infrared; OD = right eye; OS = left eye.

419

420   **Figure 5: Automatic retinal delamination interface on OCT system.** A. **Load Examination** button,
421   B. **Media Container**, showing all the OCT images, C. OCT image being selected for analysis, D.
422   **Layer Detection** button for automatic retinal layering, E. dividing line list, F. automatic
423   delamination on the retina, G. **Edit Layer** button for layered correction, H. **Save Examination**
424   button for saving the results. Scale bars = 200 μm. Abbreviation: OCT = optical coherence
425   tomography.

426

427   **Figure 6: Layered correction (A–C) and thickness measurement (D–E).** (**A**) Layered edit activation
428   interface: 1. **Edit Layer** button, 2. dividing line list (e.g., selecting all lines), 3. activated dividing
429   lines, 4. **Spacing** adjustment, 5. **Limit Range** adjustment. (**B**) Activation of a dividing line (e.g., line
430   3 in **A**), 6. line 3, the line between the inner plexiform layer and inner nuclear layer, 7. an example
431   of layering error. (**C**) Layering error modification, 8. the red circle for modification. (**D**) An example
432   of retinal lamellar thickness measurement, 9. **Measure Marker** button, 10. dividing lines of the
433   outer nuclear layer, 11. **Connect with Layer** (the measurement will connect with the layer
434   according to the dividing lines), 12. **Stay Connected on Move** (the measurement position is where
435   the manual click stays), 13. the location of the result display, 14. the measurement line
436   (perpendicular to the horizontal axis). (**E**) Measurement result acquisition, 15. the measurement
437   results (red rectangle: **Vert** value is the thickness result), 16. **Delete Marker** button for
438   measurement record deletion, 17. **New Marke**r button for remeasurement (the new result will
439   overwrite the original record). Scale bars = 200 μm.

440

Figure 7: Measurement of full retinal thickness. A. **Measure Marker** button, B. line 1 (**ILM**) and C. line 7 (**OS-RPE**) selection for showing the boundaries of the full-thickness retina, D. **Connect with Layer** selection, E. **Stay Connected on Move** selection, F. ruler bar (vertical and horizontal ruler bars, both 200 μm in length), G. measurement lines on the retina (4 lines with 200 μm of horizontal ruler length as spacing on each side of the optic papilla), H. the measurement results (the results are differentiated by different colors and correspond to the color of the measurement lines on the retina), I. Data extraction from the **Vert** value in the **Length in μm (tissue)** row. Scale bars = 200 μm. Abbreviations: ILM = inner limiting membrane; OS-RPE = photoreceptor outer segment of retinal pigment epithelium.

Figure 8: Comparison of cSLO and OCT images of *Vldlr* knockout and C57BL/6J mice. cSLO (**A**) and OCT (**B**) images of *Vldlr* knockout mice compared with the cSLO (**C**) and OCT (**D**) images of C57BL/6J mice. Characteristics of OCT in *Vldlr* knockout mice (**B**): 1) Middle reflective line (**B**, red arrows) on the inner surface of the retina with adhesion to the retinal vessel (**B**, green arrow). 2) Hyperreflective lesions, located at the subretinal space, with (**B**, white arrow) or without (**B**, yellow arrow) involvement of outer nuclear layer. The arrows on the cSLO image (**A**) represent the locations of the corresponding color arrows on OCT image (**B**). Scale bars = 200 μm. Abbreviations: cSLO = confocal scanning laser ophthalmoscope; OCT = optical coherence tomography; Vldlr = very-low-density lipoprotein receptor.

Figure 9: Mode 1: retinal paraffin sections with hematoxylin-eosin staining in *Vldlr* knockout and C57 BL/6J mouse. (**A**) An example of subretinal neovascularization invading the outer nuclear layer (thick green arrow), located in the middle part of the retina of a *Vldlr* knockout mouse. (**B**) Normal control, the middle part of the retina of a C57 BL/6J mouse. Scale bars = 50 μm. Abbreviations: Vldlr = very-low-density lipoprotein receptor; ILM = inner limiting membrane; NFL = retinal nerve fibre layer; GCL = retinal ganglion cell layer; IPL = inner plexiform layer; INL = inner nuclear layer; OPL = outer plexiform layer; ONL = outer nuclear layer; ELM = external limiting membrane; IS = photoreceptor inner segment; OS = photoreceptor outer segment; RPE = retinal pigment epithelium layer.

Figure 10: Mode 2: retinal paraffin sections with hematoxylin-eosin staining in *Vldlr* knockout and C57 BL/6J mouse. (**A**) An example of subretinal neovascularization without the involvement of outer nuclear layer (thick blue arrow) and with intact ELM (thin yellow arrow), located in the middle periphery retina in a *Vldlr* knockout mouse. (**B**) Normal control, the middle periphery retina of a C57 BL/6J mouse. Scale bars = 50 μm. Abbreviations: VLDR = very-low-density lipoprotein receptor; ILM = inner limiting membrane; NFL = retinal nerve fiber layer; GCL = retinal ganglion cell layer; IPL = inner plexiform layer; INL = inner nuclear layer; OPL = outer plexiform layer; ONL = outer nuclear layer; ELM = external limiting membrane; IS = photoreceptor inner segment; OS = outer photoreceptor segment; RPE = retinal pigment epithelium layer.

Figure 11: Comparison of retinal thickness between C57 BL/6J mice and *Vldlr* knockout mice (all data from the right eye). (**A**) Retinal thickness (μm) through the optic nerve papilla by OCT horizontal scanning. (**B**) Retinal thickness (μm) through the optic nerve papilla by OCT vertical scanning. The horizontal coordinate represents the measuring positions with spacing of 200 μm.*:

485 P < 0.05, **: P < 0.01, ***: P < 0.001. Abbreviations: T = Temporal; P = Optic papilla; N = Nasal; S
486 = Superior; I = Inferior; OCT = optical coherence tomography; VLDR = very-low-density lipoprotein
487 receptor; OD = right eye.
488
489 **DISCUSSION:**
490 In this study, OCT imaging using a small-animal retinal imaging system was applied to evaluate
491 retinal changes in *Vldlr* knockout mice, which demonstrate incomplete posterior vitreous
492 detachment, subretinal neovascularization, and retinal thickness thinning. OCT is a noninvasive
493 imaging method to examine the condition of the retina *in vivo*. Most OCT devices are designed
494 for human eye examination. The size of the hardware equipment, the setting of the focal length,
495 the setting of the system parameters, and the positioning requirements of the examinee are all
496 based on the human eye. Modifications of the lens and system settings are required to examine
497 small animals with human-specific OCT equipment. This paper presents small-animal OCT
498 examination procedures.
499
500 The focal length is different during image scanning of different small animals with different sizes
501 of eyeballs. This difference in focal length is critical and must be resolved to obtain clear and
502 accurate fundus images. One effective method is replacing the objective lens with lenses of
503 different curvatures. Due to its small eyeball, the mouse needs a contact lens of 100 D in front of
504 the cornea in addition to the double-spherical 60 D preset lens of the OCT equipment.
505
506 The OCT can only provide line scans that only cover a limited region of the retina. Therefore, it is
507 essential to standardize the protocol of OCT scans for qualitative and quantitative comparison of
508 OCT findings in different groups. Three horizontal scans and three vertical scans were performed
509 here. This machine provides a real-time cSLO image to monitor the location of the OCT scan so
510 that the position of the scan can be adjusted accurately and conveniently. Additional scans can
511 be added when an abnormal reflection is found.
512
513 The parameters of image acquisition need to be adjusted carefully. Here, it is recommended that
514 the Range Min be 0–20 and the Range Max be 50–60 (**Figure 4I,J**). When the parameters are
515 overadjusted, the signal contrast of the image would be enhanced, and the reflected signal of
516 the retina with low reflection becomes lower or even black, and some morphological information
517 will be lost.
518
519 The following are some tips to avoid image quality deterioration: 1. Place a contact lens in front
520 of the eyes immediately after anesthesia to avoid cataracts; 2. Ensure that the preset lens and
521 contact lens are clean; 3. Avoid hair entering between the cornea and the contact lens; 4. Ensure
522 the doppler, contrast, and brightness in the OCT parameters are set appropriately.
523
524 The OCT images can be used to qualitatively detect lesions and quantitatively measure metrics
525 such as retinal thickness. Here, a method is proposed to measure the retinal thickness at several
526 locations, and the average can be calculated as the mean retinal thickness. This is achieved
527 through the automatic stratification function of the OCT system. Therefore, the thickness of the
528 retinal laminations can also be measured. The measurement method is simple and accurate

529 (**Figure 6** and **Figure 7**). The results showed that the retinal thickness was lower in *Vldlr* knockout
530 mice than C57BL/6J mice, consistent with the literature[25]. The difference in retinal thickness
531 between the two groups can be clearly shown by a graph generated from the measurements at
532 multiple locations (**Figure 11**). Similar retinopathy analysis and retinal thickness measurement
533 methods have also been reported in the Stargardt disease mouse model[26]. However, it is worth
534 noting that the hyperreflective bands at the vitreous interface of the retina do not belong to the
535 retinal tissue and should be removed during stratification. In addition, if subretinal lesions invade
536 the retina, the thickness measurement should include the invaded portion.

538 This small-animal retinal imaging system has some limitations. For example, although it can
539 provide clear images of the posterior pole within 35°, image acquisition of the peripheral retina
540 is still challenging. In addition, cSLO forms a gray-scale image, which is not as good as a color
541 fundus image to detect fundus lesions (pigmentation, bleeding, exudation). Hence, further
542 improvements are needed. In summary, OCT examination by the cSLO machine could facilitate
543 the noninvasive detection and measurement of retinopathy in mouse models.

550 **DISCLOSURES:**
551 The authors declare no potential conflict of interest.

553 **REFERENCES:**
554 1. Frombach, J. et al. Serine protease-mediated cutaneous inflammation: characterization
555 of an ex vivo skin model for the assessment of dexamethasone-loaded core multishell-
556 nanocarriers. *Pharmaceutics*. **12** (9), 862 (2020).
557 2. Osiac, E., Săftoiu, A., Gheonea, D. I., Mandrila, I., Angelescu, R. Optical coherence
558 tomography and Doppler optical coherence tomography in the gastrointestinal tract. *World
559 Journal of Gastroenterology.* **17** (1), 15–20 (2011).
560 3. Xiong, Y. Q. et al. Diagnostic accuracy of optical coherence tomography for bladder
561 cancer: A systematic review and meta-analysis. *Photodiagnosis and Photodynamic Therapy*. **27**,
562 298–304 (2019).
563 4. Andrews, P. M. et al. Optical coherence tomography of the aging kidney. *Experimental &
564 Clinical Transplantation*. **14** (6), 617–622 (2016).
565 5. Terashima, M., Kaneda, H., Suzuki, T. The role of optical coherence tomography in
566 coronary intervention. *The Korean Journal of Internal Medicine*. **27** (1), 1–12 (2012).
567 6. Avital, Y., Madar, A., Arnon, S., Koifman, E. Identification of coronary calcifications in
568 optical coherence tomography imaging using deep learning. *Scientific Reports*. **11** (1), 11269
569 (2021).
570 7. Huang, D. et al. Optical coherence tomography. *Science*. **254** (5035), 1178–1181 (1991).
571 8. Tsai, T. H. et al. Optical coherence tomography in gastroenterology: a review and future
572 outlook. *Journal of Biomedical Optics*. **22** (12), 1–17 (2017).

573   9.   Chen, J. et al. Relationship between optical intensity on optical coherence tomography
574   and retinal ischemia in branch retinal vein occlusion. *Scientific Reports*. **8** (1), 9626 (2018).

575   10.   Chen, X. et al. Quantitative analysis of retinal layer optical intensities on three-
576   dimensional optical coherence tomography. *Investigative Opthalmology & Visual Science*. **54**
577   (10), 6846–6851 (2013).

578   11.   Cruz-Herranz, A. et al. Monitoring retinal changes with optical coherence tomography
579   predicts neuronal loss in experimental autoimmune encephalomyelitis. *Journal of*
580   *Neuroinflammation*. **16** (1), 203 (2019).

581   12.   Podoleanu, A. G. Optical coherence tomography. *Journal of Microscopy.* **247** (3), 209–219
582   (2012).

583   13.   Augustin, M. et al. Optical coherence tomography findings in the retinas of SOD1
584   knockout mice. *Translational Vision Science & Technology*. **9** (4), 15 (2020).

585   14.   Berger, A. et al. Spectral-domain optical coherence tomography of the rodent eye:
586   highlighting layers of the outer retina using signal averaging and comparison with histology. *PLoS*
587   *One*. **9** (5), e96494 (2014).

588   15.   Burns, M. E. et al. New developments in murine imaging for assessing photoreceptor
589   degeneration in vivo. *Advances in Experimental Medicine & Biology.* **854**, 269–275 (2016).

590   16.   Jagodzinska, J. et al. Optical coherence tomography: imaging mouse retinal ganglion cells
591   in vivo. *Journal of Visualized Experiments: Jove*. (127) 55865 (2017).

592   17.   Kocaoglu, O. P. et al. Simultaneous fundus imaging and optical coherence tomography of
593   the mouse retina. *Investigative Opthalmology & Visual Science*. **48** (3), 1283–1289 (2007).

594   18.   Tode, J. et al. Thermal stimulation of the retina reduces Bruch's membrane thickness in
595   age related macular degeneration mouse models. *Translational Vision Science & Technology*. **7**
596   (3), 2 (2018).

597   19.   Wang, R., Jiang, C., Ma, J., Young, M. J. Monitoring morphological changes in the retina of
598   rhodopsin-/- mice with spectral domain optical coherence tomography. *Investigative*
599   *Ophthalmology & Visual Science*. **53** (7), 3967–3972 (2012).

600   20.   Xie, Y. et al. A spectral-domain optical coherence tomographic analysis of Rdh5-/- mice
601   retina. *PLoS ONE*. **15** (4), e0231220 (2020).

602   21.   Li, Q. et al. Noninvasive imaging by optical coherence tomography to monitor retinal
603   degeneration in the mouse. *Investigative Ophthalmology & Visual Science*. **42** (12), 2981–2989
604   (2001).

605   22.   Horio, N. et al. Progressive change of optical coherence tomography scans in retinal
606   degeneration slow mice. *Archives of Ophthalmology*. **119** (9), 1329–1332 (2001).

607   23.   Hu, W. et al. Expression of VLDLR in the retina and evolution of subretinal
608   neovascularization in the knockout mouse model's retinal angiomatous proliferation.
609   *Investigative Opthalmology & Visual Science*. **49** (1), 407–415 (2008).

610   24.   Wyne, K. Expression of the VLDL receptor in endothelial cells. *Arteriosclerosis,*
611   *Thrombosis, and Vascular Biology*. **16** (3), 407–415 (1996).

612   25.   Augustin, M. et al. In vivo characterization of spontaneous retinal neovascularization in
613   the mouse eye by multifunctional optical coherence tomography. *Investigative Opthalmology &*
614   *Visual Science*. **59** (5), 2054–2068 (2018).

615   26.   Fang, Y. et al. Fundus autofluorescence, spectral-domain optical coherence tomography,
616   and histology correlations in a Stargardt disease mouse model. *The FASEB Journal*. **34** (3), 3693–
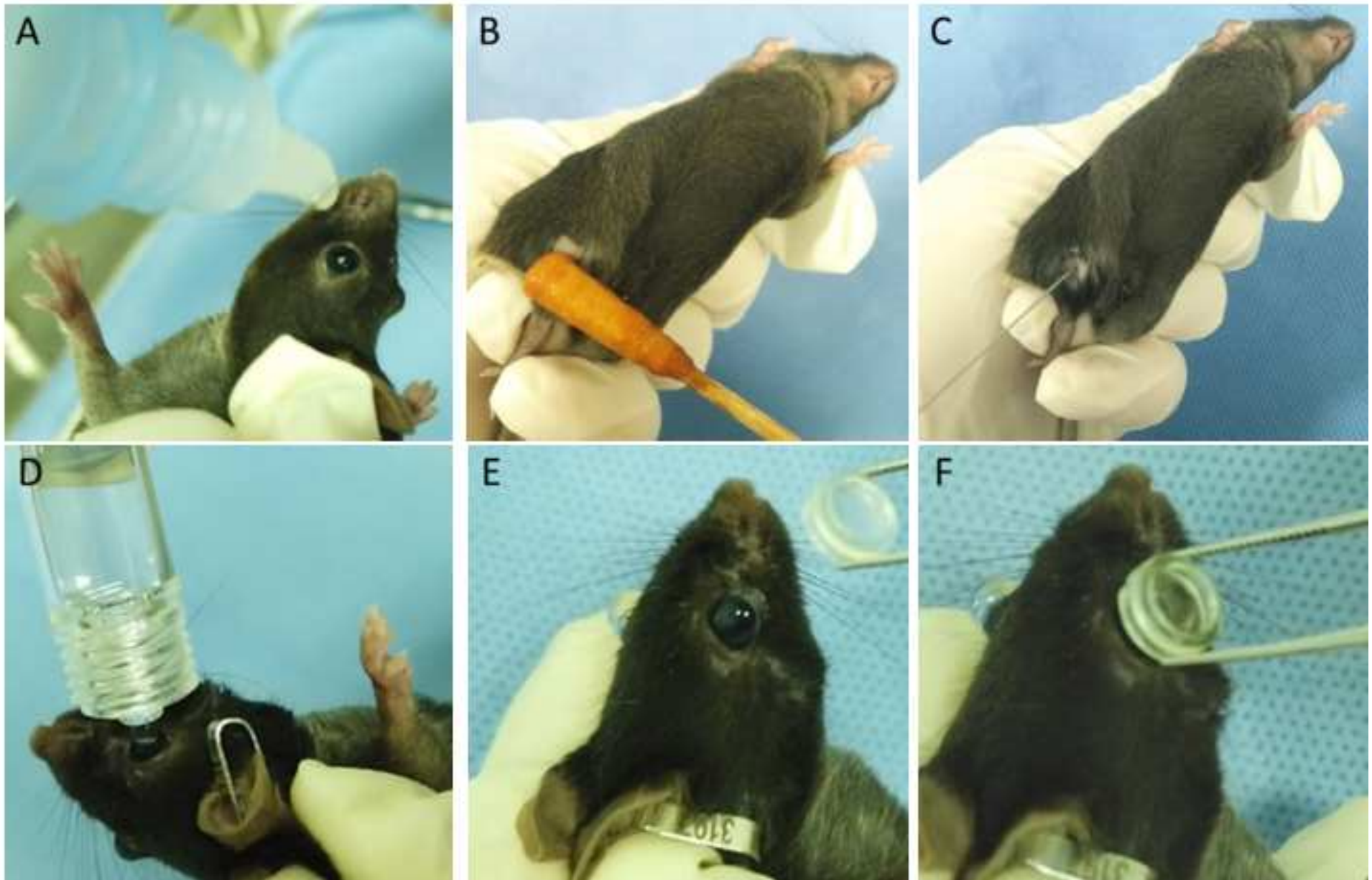
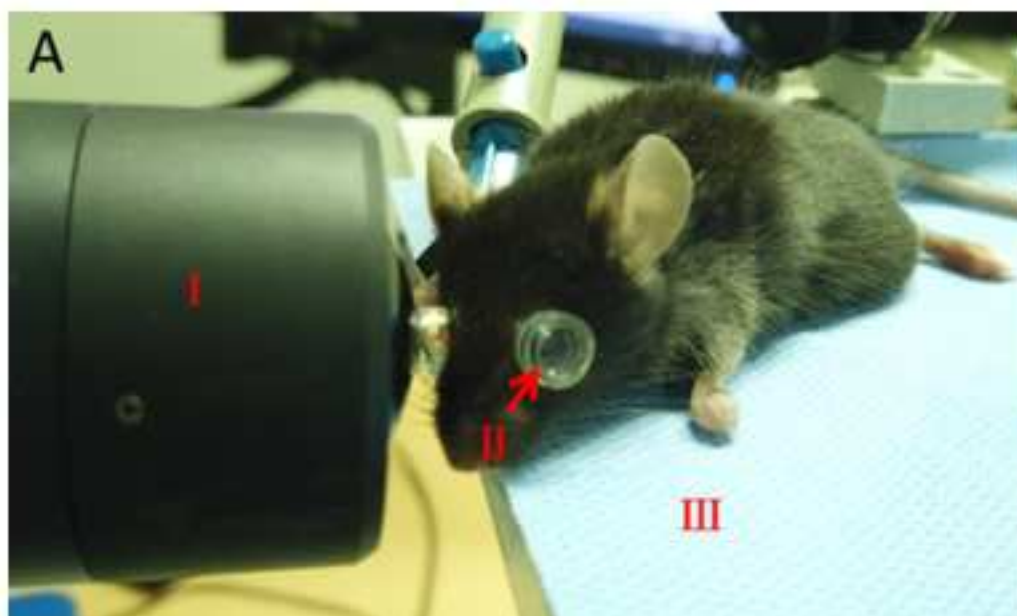617   3714 (2020).

618

Figure 1 Click here to access/download;Figure;Figure-1.tif

Figure 2
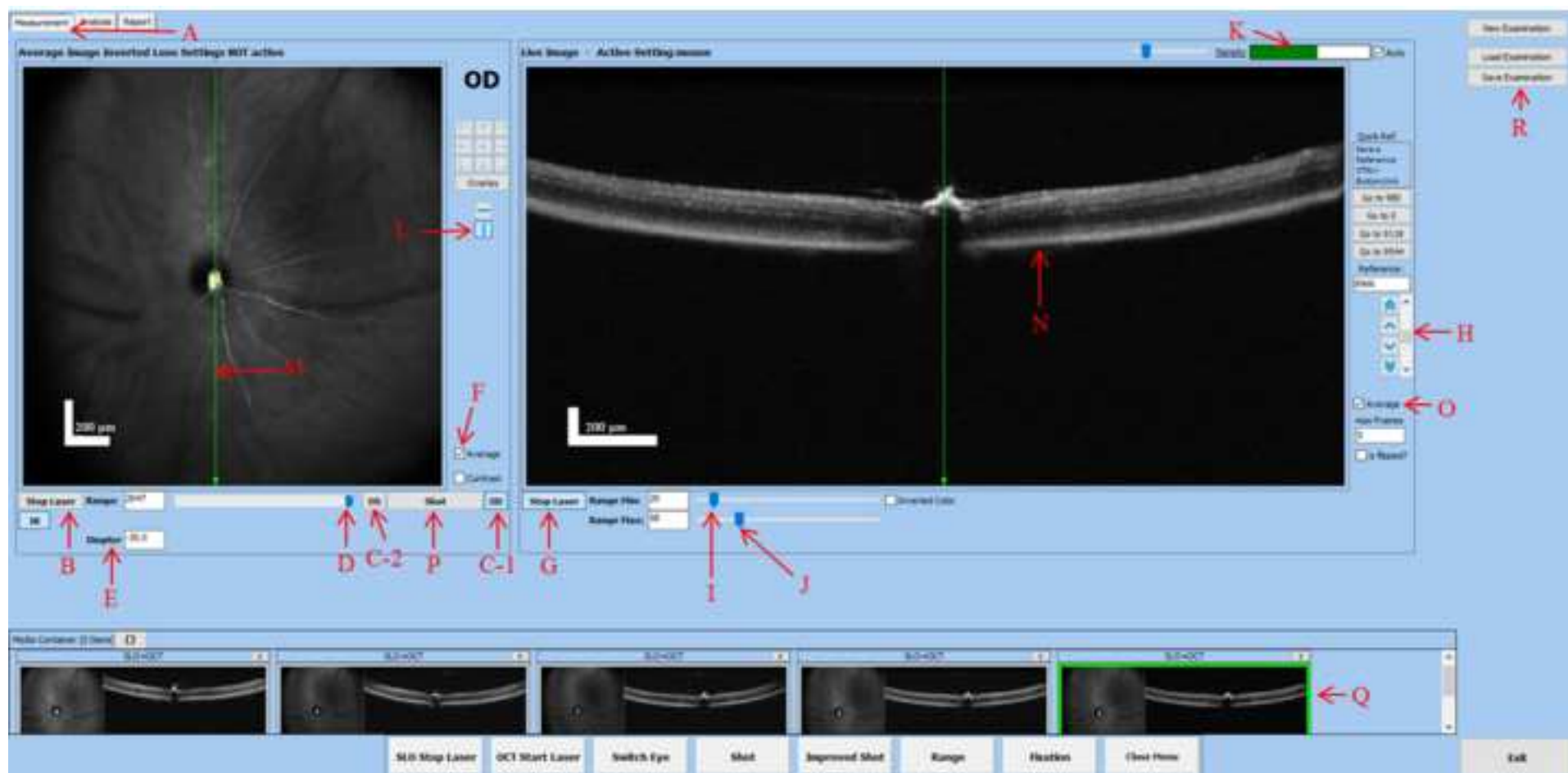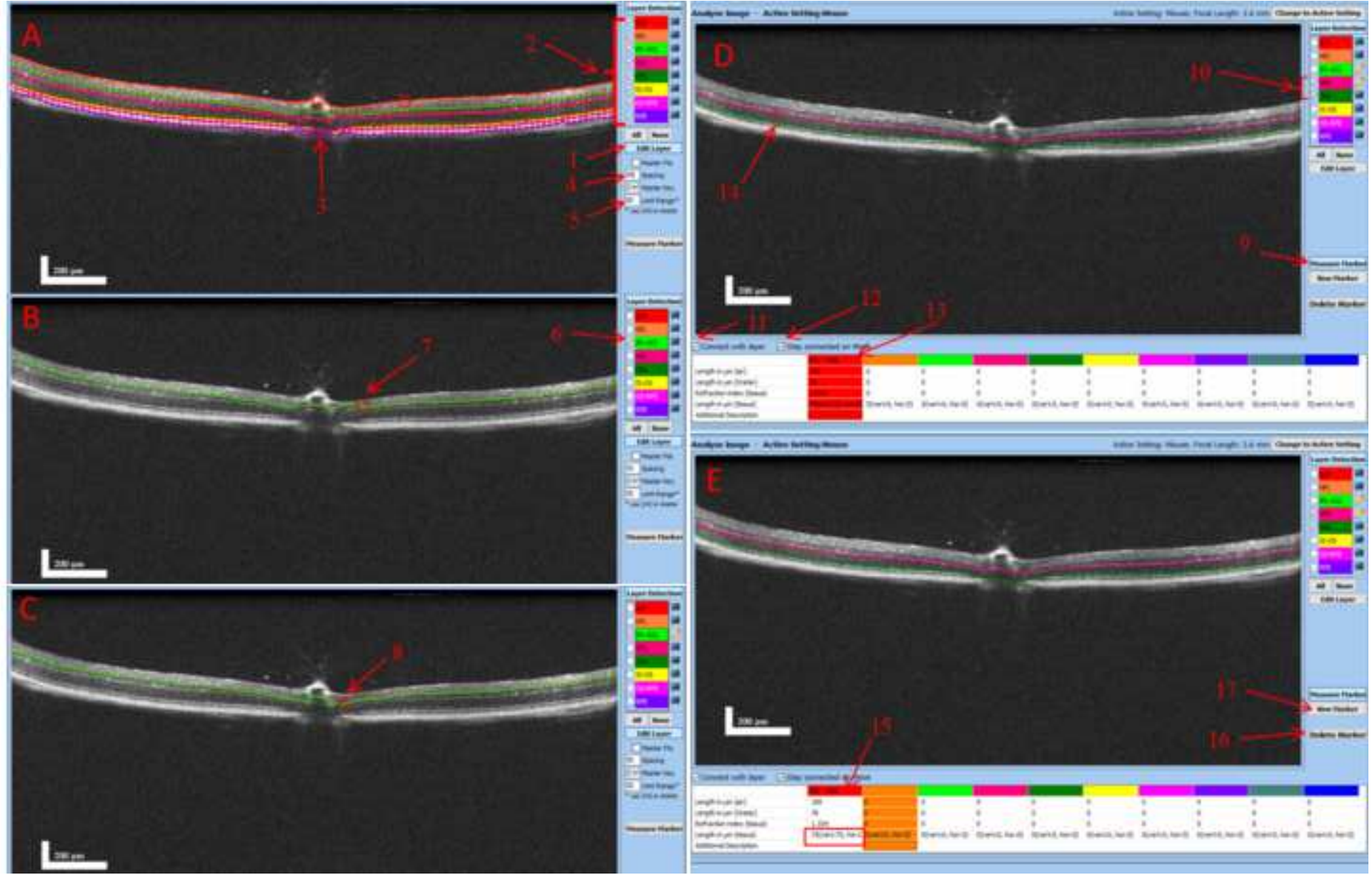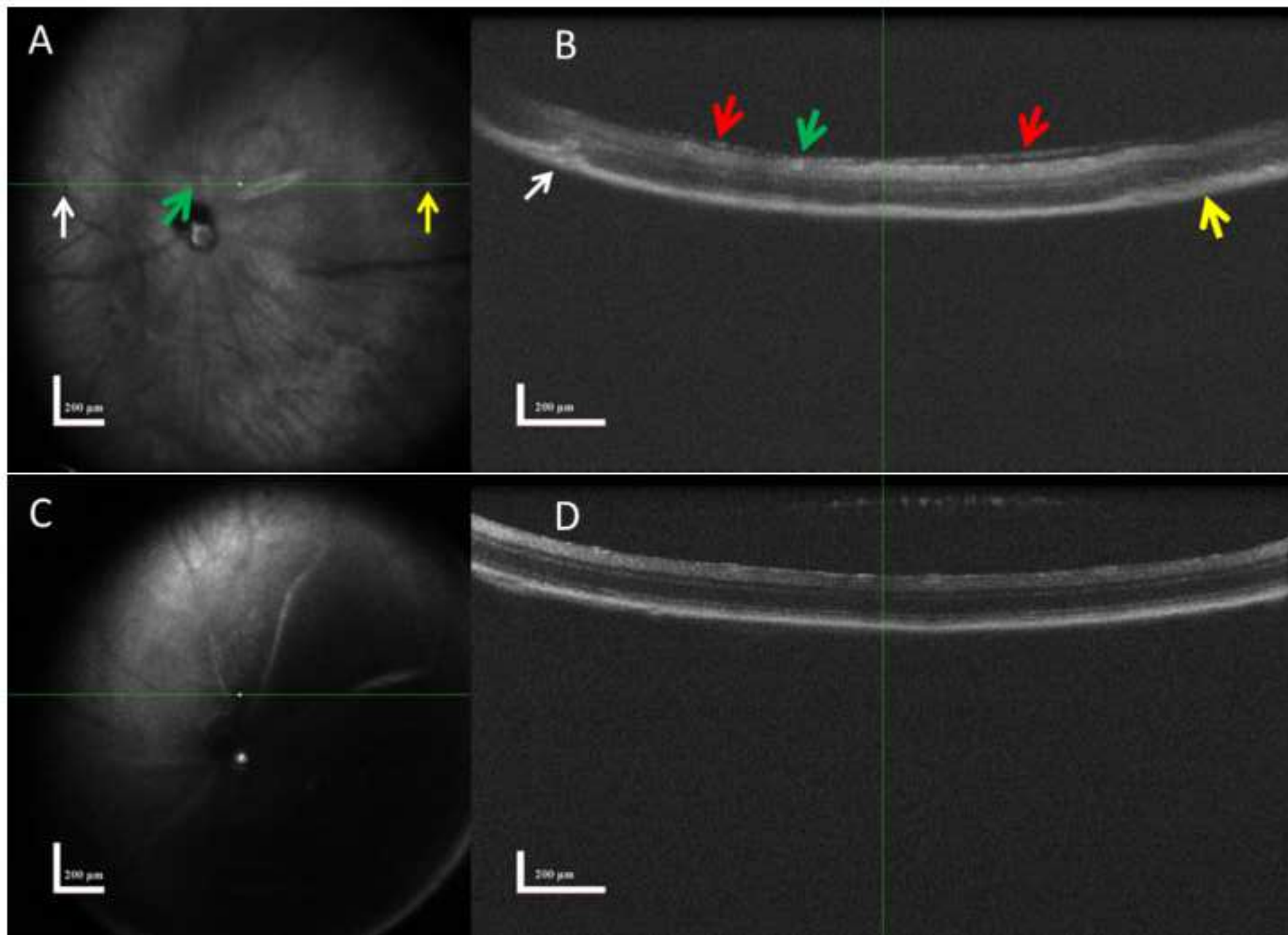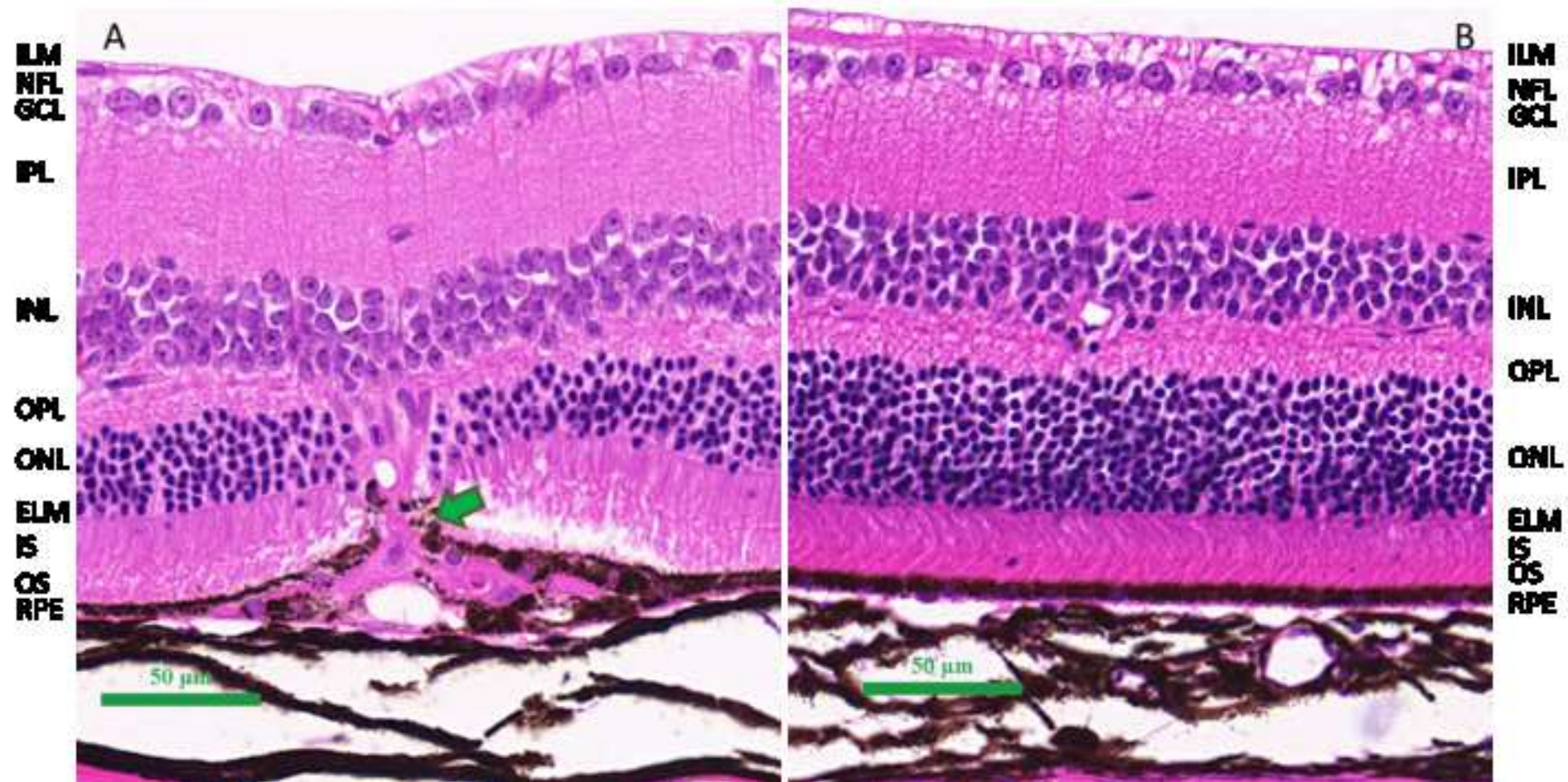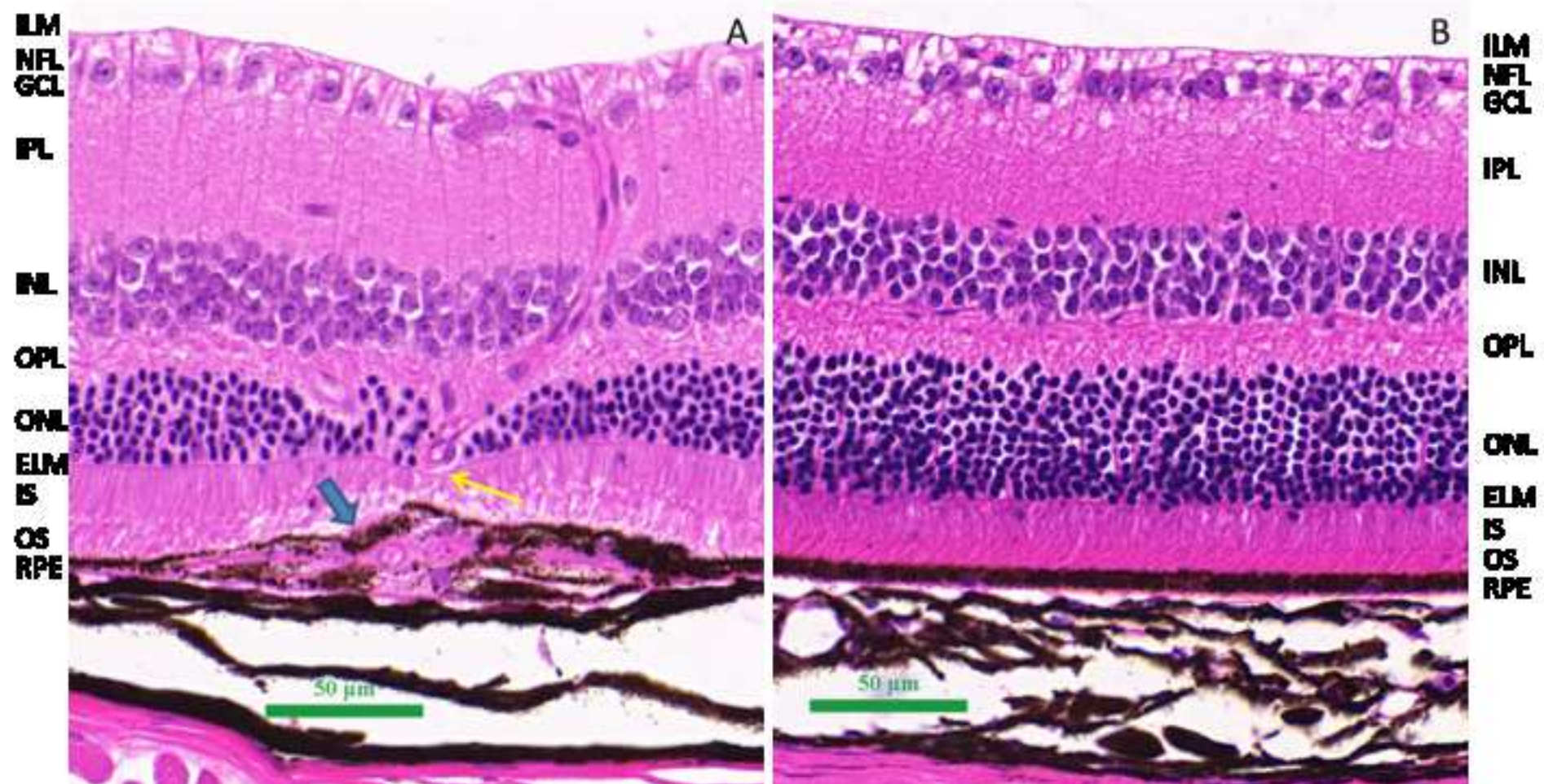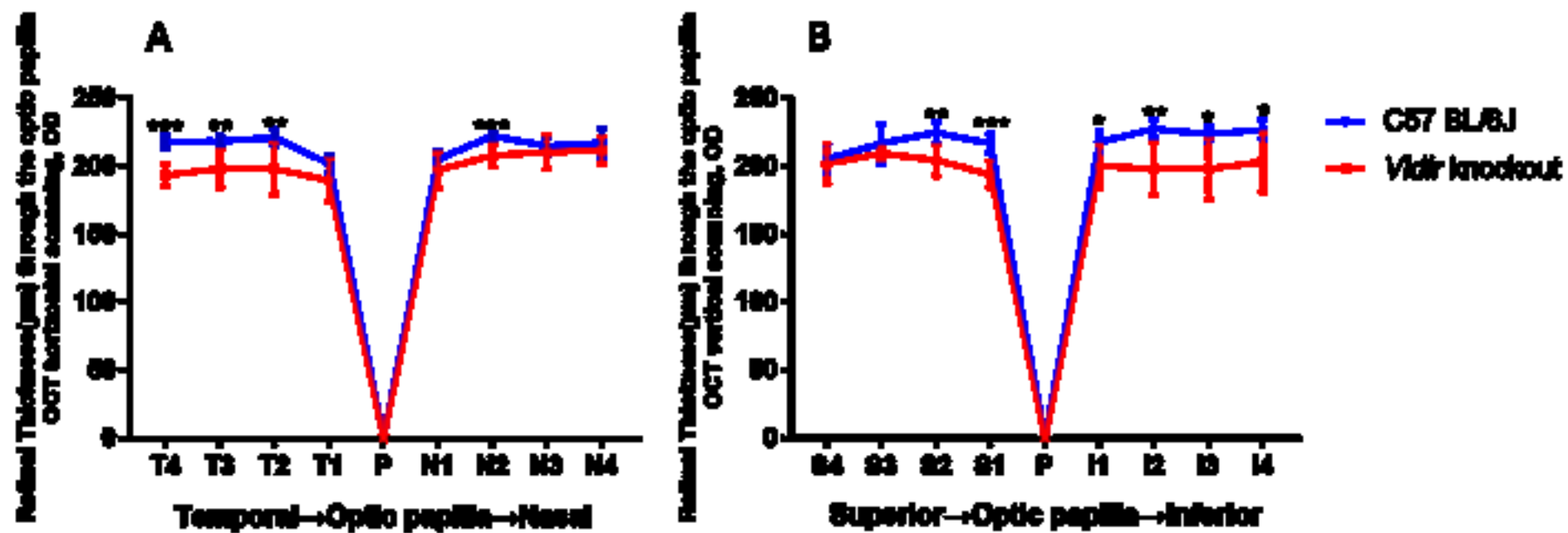
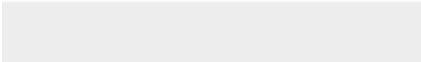Click here to access/download;Figure;Figure-2.tif ⬇

Figure 3

Click here to access/download
Table of Materials
JoVE_Materials-OCT (2).xls

Dear Editor,

We appreciate the important comments raised by the reviewers and editor. These comments helped

us a lot to improve our manuscript. We have revised the manuscript accordingly. Please see below

for a point-by-point response to the comments.

Best,

Xiaoting Mai

Editorial comments:

Editorial Changes

Changes to be made by the Author(s):

1. Please take this opportunity to thoroughly proofread the manuscript to

ensure that there are no spelling or grammar issues.

The spelling and grammar issues have been thoroughly proofread.

2. For in-text formatting, corresponding reference numbers should appear as

numbered superscripts after the appropriate statement(s) and before the

punctuation.

The corresponding reference numbers have been modified to numbered

superscripts form, and placed after the appropriate statement(s) and before the

punctuation.

3. Please also include in the Introduction the following with citations:

a) A clear statement of the overall goal of this method

Here, we demonstrated the application of OCT imaging to detect retinal

lesions in VLDLR knockout mice, hoping to provide some technical reference for

the research of retinopathy in small animal models. (*Page 1, line 64-66*)

b) The rationale behind the development and/or use of this technique

The principle of OCT is optical coherence reflectometry, which obtains tissue cross-sectional information from the coherence of light reflected from a sample and converts it into graphic or digital form through a computer system. The reference literature is: *Huang, D., et al., Optical coherence tomography. Science (New York, N.Y.), 1991. 254(5035): p. 1178-81.* (*Page 2, 42-44*)

c) The advantages over alternative techniques with applicable references to previous studies

Compared to the OCT which was first used for retinal imaging in mice, OCT in small animals has now been optimized in both hardware and software systems. For example, OCT in combination with the tracker significantly reduces the signal noise ratio, OCT software system upgrades allow more retinal layers to be detected automatically, and the integrated DLP beamer helps to reduce the motion artifacts. (*Page 2, 54-58*)

d) A description of the context of the technique in the wider body of literature

Optical coherence tomography (OCT) is an imaging technique that can provide in vivo high resolution, cross-sectional imaging for tissue[1-9], especially the non-invasive examination in retina[10-13].(*Page1-2, 39-41*)

e) Information to help readers to determine whether the method is appropriate for their application

The method providing here is for the technical reference in the research of retinopathy in small animal models. It also is our goal here. The information has

been added. (*Page 2, 65-66*)

4. The Protocol should be made up almost entirely of discrete steps without large paragraphs of text between sections. The Protocol should contain only action items that direct the reader to do something.

The Protocol has been modified as discrete steps. (*Page 2-7, 68-328*)

5. JoVE cannot publish manuscripts containing commercial language. This includes trademark symbols (™), registered symbols (®), and company names before an instrument or reagent. Please remove all commercial language from your manuscript and use generic terms instead. All commercial products should be sufficiently referenced in the Table of Materials.
For example: Image-Pro Plus, Excel, etc.

All commercial language has been expunged from the manuscript, including logos that can be clearly seen in the picture, e.g., Figure 4 and Figure 5 in the original article, and the software name (Image-Pro Plus, Excel).

6. Please adjust the numbering of the Protocol to follow the JoVE Instructions for Authors. For example, 1 should be followed by 1.1 and then 1.1.1 and 1.1.2 if necessary.

All the numberings have been adjust. (*Page 2-7, 72-328*)

7. Please revise the text to avoid the use of any personal pronouns (e.g., "we", "you", "our" etc.).

All personal pronouns have been expunged from the manuscript (all the words of "we", "you" or "our").

8. Please ensure that all text in the protocol section is written in the imperative tense as if telling someone how to do the technique (e.g., "Do this," "Ensure that," etc.). The actions should be described in the imperative tense in complete sentences wherever possible. Avoid usage of phrases such as "could be," "should be," and "would be" throughout the Protocol. Any text that cannot be written in the imperative tense may be added as a "Note." However, notes should be concise and used sparingly.

All text in the protocol section is written in the imperative tense in complete sentences. We didn't use the phrases such as "could be," "should be," or "would be" in the Protocol. (*Page 2-7, 72-328*)

9. Please add more details to your protocol steps. Please ensure you answer the "how" question, i.e., how is the step performed?

Yes, we have add more details to the protocol steps. For example, *page 2,80-83*; *page 3, 93-100*; *page 4, 140-163*.

Line 92: The Mydriatic preparation has no steps associated. Please check.

The mydriatic drop doesn't have to be configured. It's a whole bottle. We have explained it in the article. (*Page 3, 124*)

Line 96: Was a pre-determined quantity of eye drop administered? If yes, please specify.

Yes. It has been specified. (*Page 3, 124*)

Line 104: What was the volume used in the current protocol?

The volume has been added in the protocol. It is one drop each eye. (*Page 4, 129*)

Line 106: Syringe size used.

The syringe size has been added in the protocol. It is a 50μl microsyringe. (*Page 4, 144*)

Line 110: Were the hair removed? Was the disinfection done once? Usually, 3 rounds of disinfection are done.

Yes, the localized hair was removed to expose the thigh muscles. We will disinfect the skin 3 times with povidone-iodine. (*Page 4, 149-151*)

Line 111: What does 0.3 cm denote? Is it the depth of injection?

Yes. It is the depth of injection. It has been added. (*Page 4, 154*)

Line 115: How was proper anesthetization confirmed?

Inject all anesthetic solution in the microsyringe (smooth injection with no spillover indicates successful operation). (*Page 4, 157-158*)

Line 117,185: What does Dpt, RPE stand for? Please specify/expand.

The word "Dpt" should be "D". It's a diopter unit, standing for the Lens diopter. We have revised it. (*Page 5, 173-175*)

And we also expand "OS" and "RPE". OS: photoreceptor outer segments;

RPE: Retinal pigment epithelial layer. (*Page 8, 318-319*)

Line 148: What does lesion site mean here?

The word "lesion site" means abnormal reflection site. We have change the word. (*Page 6, 254*)

10. Please include a single line space between each step, substep, and note in the protocol section. Please highlight up to 3 pages of the Protocol (including headings and spacing) that identifies the essential steps of the protocol for the video, i.e., the steps that should be visualized to tell the most cohesive story of the Protocol. Remember that non-highlighted Protocol steps will remain in the manuscript, and therefore will still be available to the reader.

We have added a single line space between each step, substep, and note in the protocol section. We have highlight the Protocol that identifies the essential steps of the protocol for the video. (*Page 2-8, 68-330*)

11. Please do not number the results section.

The numbers in the results section have been deleted.

12. Please explain the Representative Results in the context of the technique you have described, e.g., how do these results show the technique, suggestions about how to analyze the outcome, etc.

Yes, we have an explanation for that. (*Page 8, 333-334; page 9, 357-358*)

13. Please remove all the embedded figures and table from the manuscript.

We have removed all the embedded figures and table from the manuscript.

14. Please provide a scale bar for all images captured using a microscope.

The images captured using a microscope have had the scale bar. We have shown the scale bar in the bright color. However, in pictures that are not taken under a microscope, objects have different distances and scales, making it impossible to set up a unified bar. (Figure.4-8)

15. Please use capital letters for various image panels.

We have use capital letters for various image panels. (Figure.1-3,6,8)

16. As we are a methods journal, please also include in the Discussion the following in detail along with citations:

a) Critical steps within the protocol

We have listed above in the discussion section. (*Page.11, 454-457, 469-473*)

b) Any limitations of the technique

We have listed above in the discussion section. (*Page.12, 482-485*)

c) The significance with respect to existing methods

We have listed above in the discussion section. (*Page.12, 486-487*)

17. Please ensure that the references appear as the following: [Lastname, F.I., LastName, F.I., LastName, F.I. Article Title. Source. Volume (Issue), FirstPage – LastPage (YEAR).]

All references conform to the prescribed format. (Page.12-14, 496-563)

Reviewer #1:

Manuscript Summary:

the images of both groups showed retinal layers.

Major Concerns:

None

Minor Concerns:

Do you think you could detail the installation of the 60 Dpt. double spherical lens (objective lens) on the cSLO device?

The 60D lens has spiral interface, rotary mount, as seen in Figures 1 and 3. (*Page.5, 173*)

Could you please add a statistical comparison of retinal thickness between groups?

Yes, we have added the statistical comparison of retinal thickness between groups. (*Page.9, 359-362*, and Figure.9)

Clinical OCT images provide a signal strength information. Does the OCT used in this study device measure it?

Yes, the OCT used in this study shows the signal strength information when operating. It is showed as signal intensity of the image. (*Page.9,385-386*, Figure 4.①)

Reviewer #2:

Manuscript Summary:

The manuscript entitled "Application of Optical Coherence Tomography in a Mouse Model of Retinopathy" describes the authors' study of OCT analysis using VLDLR KO mice. In the manuscript, although the authors described detailed protocols of their experiment, several parts should be pointed out as preliminary portions that may need to be corrected, if possible.

Major Concerns:

1. The purpose of the study is quite ambiguous. If the purpose of this study is to introduce the methods and results of OCT analysis using mouse models, there is no new information that should be added to what we have already known, because there are numerous publications dealing with OCT analyses using rodent models in addition to what were cited by the authors shown in the reference list. Conversely, if the purpose of the study is to show the novel OCT findings of the VRDLR KO mice, the results presented in Figure 6 do not provide sufficient level of information that would make readers satisfied. The reasons of this latter comment are described in the following column.

JOVE is mainly about detailing the steps of a method, not about getting new results, or building new methods. Therefore, the purpose of the study is to provide some technical details. (*Page.2, 64-66*)

2. Because the authors mentioned that OCT is well correlated with histopathology, there is no evidence that proves the correlation of the OCT findings obtained in the experiment to their histopathologic findings in the text. To scientifically improve quality of the manuscript, the authors need to present histopathologic findings corresponding to the subretinal band with high refractive lesion ("neovascularization"), so that we can more precisely compare the presented OCT findings in relation to histopathology.

3. In Table 1 and comments in L217-218 (P.6), no statistical analysis was performed. It is not scientific at all.

We have added the statistical analysis and improved this part. (*Page.9, 359-362*, Figure.9)

4. What is the purpose of analyzing the whole retinal thickness? Why didn't you perform retinal sublayer thickness analysis in addition to the whole thickness measurement? Because sublayer segmentation analysis is one of advantages of using OCT, the authors should consider it.

Yes, we have considered it and added the sublayer segmentation analysis using the OCT. (*Page.7-8, 261-327*, Figure.5-7)

5. In the retinal thickness analysis (Figure 5), two or three Nos. 8 and 10 straight lines do not appear perpendicular to the retina in the peripheral portion, so that they do not reflect the real thickness of the retina using these oblique lines. Isn't it a limitation of this measurement procedure?

In thickness analysis, the straight line is perpendicular to the horizontal axis rather than the retina, which is a characteristic of OCT image analysis. In addition, we have changed the original analysis method to use the built-in analysis function on the system. (*Page.7-8, 261-327*, Figure.5-7)

Minor Concerns:

1. In Figure 6. b and comments in L207-215 (P.5-6), why does the same Figure 6. B appear in both vertical development mode and horizontal expansion mode?

It sounds logically impossible.

We wrote the numbers together, which caused confusion, and now the problem is solved. (*Page.10,421-428*)

2. In Figure 4 legend in L251 (P.8), isn't scanning direction of No.11 in Figure 4 actually "vertical" instead of "horizontal"?

Yes, vertical scanning is selected in the picture. It has been revised. (*Page.9, 386-387*, Figure.4)

Reviewer #3:

Manuscript Summary:

The manuscript describes the protocol of imaging mouse retina using a commercial OCT. The authors use the protocol to image and compare the difference between retinas of normal and very-low-density lipoprotein receptor knockout mice. The manuscript is well organized, all materials and equipment are listed, and the steps in the protocol are clear and easy to follow.

Major Concerns:

The manuscript is well written and well organized, I don't have major concerns.

Minor Concerns:

The authors demonstrate the protocol by imaging normal and retinopathy retina. Such protocol also applies to many other studies that involve imaging retinas of different disease model. Maybe the authors could discuss the broader application. Another minor suggestion is for the authors to provide tips that help avoid pitfalls that could lead to bad image.

we've added some tips in the discussion. (*Page.11, 463-467*)